Nematic Braids: Topological Invariants and Rewiring of Disclinations

Simon Čopar[1] and Slobodan Žumer[1,2]
[1]Faculty of Mathematics and Physics, University of Ljubljana, Jadranska 19, 1000 Ljubljana, Slovenia
[2]Jožef Stefan Institute, Jamova 39, 1000 Ljubljana, Slovenia
(Received 9 September 2010; published 28 April 2011)

The conventional topological description given by the fundamental group of nematic order parameter does not adequately explain the entangled defect line structures that have been observed in nematic colloids. We introduce a new topological invariant, the self-linking number, that enables a complete classification of entangled defect line structures in general nematics, even without particles, and demonstrate our formalism using colloidal dimers, for which entangled structures have been previously observed. We also unveil a simple rewiring scheme for the orthogonal crossing of two $-1/2$ disclinations, based on a tetrahedral rotation of two relevant disclination segments, that allows us to predict possible nematic braids and calculate their self-linking numbers.

DOI: 10.1103/PhysRevLett.106.177801 PACS numbers: 61.30.Jf, 61.30.Dk, 82.70.Dd

Depending on the temperature and their molecular properties, nematogenic media can form isotropic, nematic, chiral, nematic, or even blue phases, each characterized by a specific orientational ordering of the constituent molecules. Their anisotropic nature allows the formation of disclinations that can be stabilized by geometric or intrinsic constraints. Recently, a lot of progress has been made on the stabilization and manipulation of disclinations by using dispersions of colloidal particles [1–4] or confinement to porous networks [5]. In nematic dispersions, the anisotropic interparticle interactions mediated by elastic deformations and defects lead to diverse colloidal structures that promote self-assembly and offer great potential for photonics and plasmonics [6]. Nematic braids are disclination networks where defect loops are not localized around one particle, but instead entangle clusters of particles [7,8]. The existence of entangled structures was first proposed based on the results of numerical simulations [9,10]. They have since been observed experimentally and their stability has been extensively analyzed [7,11]. These structures are not sufficiently well described by the theory developed for simple nematic defects [12] and a complete theoretical understanding is still lacking. Nematic braids may also include knots and links [13], otherwise seen in the physics of polymers [14], DNA [15–17], and knotted light [18]. Easy experimental observation of nematic disclination networks, and their rewiring, knotting, and linking by laser tweezers [7,13], places nematic braids as a primary template for the study of nontrivial topology in physical systems.

Nematic braids stabilized by homeotropic particles consist of closed $-1/2$ disclination loops. To fully describe a single disclination loop, we generalize the mathematical notion of a loop by introducing the self-linking number, which counts how many times the cross section of the disclination turns during a complete loop. This invariant applies to elastic loops, DNA loops [17], and other fields, but in the case of a $-1/2$ nematic disclination, due to its intrinsic threefold symmetry, it assumes specific fractional values, similar to flux discretization in the fractional quantum Hall effect [19].

For the investigation of the self-linking number, we chose a colloidal dimer consisting of two spherical particles with strong homeotropic anchoring, confined to a homogeneous planar nematic cell [7]. Depending on the particle size, confinement, and initial conditions, the particles can interact by arranging themselves into dipolar or quadrupolar structures [2], or they can be bound by $-1/2$ disclination loops shared between both particles [11]. The homogeneous director field environment energetically disfavors linking and knotting, which reveals the more basic rewiring properties of entangled states.

We demonstrate that differences between dimer structures are localized to tetrahedral regions around crossings of disclinations (Fig. 1), from which we derive rules for calculating the self-linking number and classifying all dimer structures. The rewiring rules apply to structures involving $-1/2$ disclinations in any confinement and can be used to predict and design nematic braids consisting of complex linked and knotted loops.

We start by examining the similarities of two dimer disclination configurations [11]. The ''entangled hyperbolic defect structure'' (referred to as the theta structure from here on) is the only dimer structure with space inversion symmetry and consists of two perpendicular loops, one encircling both particles and the other placed symmetrically between them [Fig. 1(a)]. The ''omega structure,'' on the other hand, consists of a single loop wrapped around both particles and has two chiral isomers [Figs. 1(b) and 1(c)]. All three structures have similar director field and line geometry at the far ends of the colloidal particles and along the vertical axis (Fig. 5 in [11]). They only differ in the way the left arc, right arc, and central loop meet between the particles [see the encircled

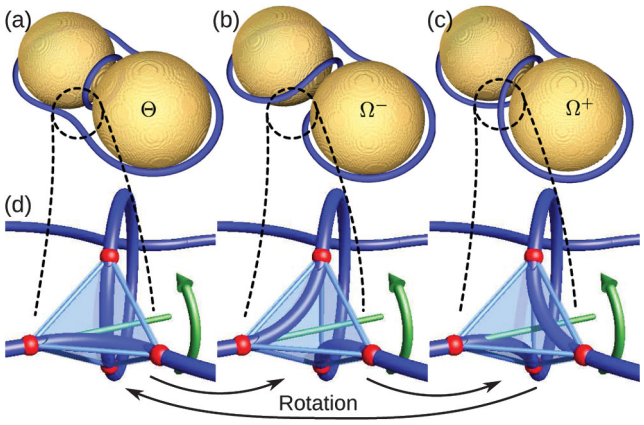

FIG. 1 (color). Rewiring sites of different dimer structures. (a)–(c) Theta structure and two chiral omega structures (simulations by Ravnik [7]). Rewiring sites are marked and paired with corresponding idealized structures. (d) The three conformations of a disclination crossing with tetrahedral symmetry. Rewiring is performed by rotating around a C_3 symmetry axis of the tetrahedron.

areas on Figs. 1(a)–1(c)]. The conversion of one structure into another is achieved by rewiring the crossing, while leaving the remote field intact, which requires a cutting of disclinations. The resulting four end points define a tetrahedron that encloses the rewiring site. Inside the tetrahedron, two perpendicular disclination segments connect pairs of the four vertices [Fig. 1(d)]. Experimentally, rewiring is achieved by local laser melting of a nematic [13].

The threefold symmetry of $-1/2$ disclinations (Fig. 2) entering the tetrahedron through the vertices coincides with the C_3 tetrahedral symmetry axes. The director field inside the tetrahedron has intrinsic dihedral symmetry (D_{2d}), ensured by the relative positioning of the disclinations. Because of this symmetry and the profile of the disclinations, the director field stands perpendicularly to all the faces of the tetrahedron and makes hyperbolic turns at all the edges, thus completing the full tetrahedral

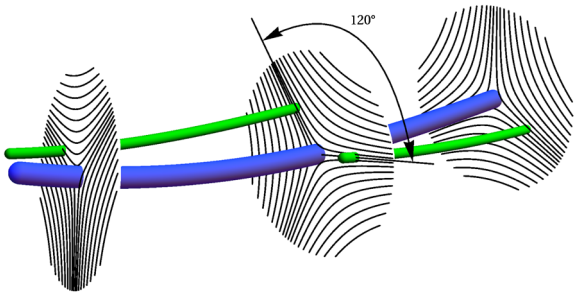

FIG. 2 (color online). To describe a disclination line, we introduce a ribbon, defined by an axis curve and a secondary curve that follows the orientation of the field cross section of the disclination. The ribbon may reconnect with itself with an offset angle of $\pm 120°$ while keeping the director field continuous, due to the symmetry of its cross section.

symmetry of the director field on the surface of the tetrahedron. Consequently, rotations from the tetrahedral symmetry group preserve the continuity of the disclination lines and the surrounding director field and therefore always generate physically possible structures. As the disclination segments inside the tetrahedron have lower symmetry (D_{2d}) than the field on its surface, rotations around a chosen C_3 symmetry axis generate 3 distinct configurations of disclinations, depicted in Fig. 1(d).

The real director field deviates from perfect tetrahedral symmetry in order to accommodate the proximity of the particles and to minimize the free energy. However, it only differs from the idealization by a continuous transformation, so the topological invariants are not affected. In further derivations, we assume this symmetry to be exact.

The director field surrounding a disclination may rotate around the disclination line tangent. In a closed loop, rotations are restricted by the fact that the director field must be continuous. The loop, together with the orientation of its cross section, can be described mathematically by a ribbon (Fig. 2). A ribbon can be assigned a self-linking number Sl a topological invariant that labels how many times it turns around its tangent in the course of one loop. Because of the three fold symmetry of disclinations, the self-linking number is not restricted to integers, but can assume any third-integer value (Fig. 2). Using Călugăreanu theorem, we can decompose the self-linking number into writhe and twist [20,21],

$$\mathrm{Sl} = \mathrm{Wr} + \mathrm{Tw}. \tag{1}$$

Writhe depends on how the loop changes direction in space, while twist contains information about the local torsion of the ribbon around its axis. Consider the theta structure [Fig. 1(a)]. Up to an arbitrary homotopic transformation, the structure is completely symmetric and both loops are planar. Both twist and writhe therefore equal zero, which can be verified using the corresponding Gauss integral definitions [20,22]. Tetrahedral rotation of a portion of the ribbon does not change the twist, as it is defined as an integral of local twist density, which is preserved by rigid transformations. As we have shown that the theta structure has zero twist, the same holds for all entangled dimer structures. It follows from Eq. (1) that in this idealization the self-linking number equals the writhe. The physics of nematic liquid crystals is hidden in the transformation rules for rewiring and is not involved in the computation of writhe, which only depends on the disclination loop geometry.

In practice, disclination loops do not necessarily have zero twist, but this can always be changed by continuous transformations that preserve the topology of the structure. The twist and writhe convert into each other under such transformations, but their sum remains equal to the self-linking number, calculated in our idealized case.

Since the writhe only depends on the axis curve of a ribbon, ordinary loops can be used instead of ribbons. We use the tantrix representation: the loop is mapped to the unit sphere of tangents. Fuller's formula [16] expresses writhe in terms of the spherical area A enclosed by the tangent indicatrix (tantrix) loop. The writhe given by this formula has modulo 2 ambiguity because full 4π wraps do not change the tantrix loop,

$$\mathrm{Wr} = \frac{A}{2\pi} - 1 \bmod 2. \tag{2}$$

The tetrahedral rotations change which pairs of the vertices are connected by segments of the disclination loop. Each loop segment is planar and maps to a great circle arc on the tantrix sphere [Fig. 3(a)]. The end points of these arcs are the tangents through the vertices of the tetrahedron, which form a square on the tantrix sphere. Rewiring induced by the tetrahedral rotation changes the enclosed area by $\mp 4\pi/6$, which by Fuller's formula (2) corresponds to a $\pm 2/3$ change in writhe. This is consistent with the restriction of the self-linking number to thirds, imposed by the symmetry of $-1/2$ disclinations (Fig. 2). It can be shown that the modulo 2 ambiguity in Eq. (2) can be dropped in our case [22]. As the tangents flip sign if the parametrization of a curve is reversed, the $\pm 2/3$ change in writhe is correct only for tetrahedral rotations that preserve continuous parametrization of the loops. If this is not the case, the change in writhe can be calculated by finding a succession of multiple rewirings that result in the same structure [Fig. 3(b)].

We can generalize the notion of writhe for a union of two or more loops A_i that may or may not be linked. The Gauss integral that defines writhe decomposes into writhes of individual loops, which equal self-linking numbers, $\mathrm{Sl}(A_i)$, and linking numbers $\mathrm{Lk}(A_i, A_j)$ between pairs of loops [22]

$$\mathrm{Wr}(A_0 \cup \cdots \cup A_n) = \sum_i \mathrm{Sl}(A_i) + 2\sum_{i>j} \mathrm{Lk}(A_i, A_j). \tag{3}$$

Combining this with the fact that every parametrization-preserving rewiring changes the total writhe by $\pm 2/3$ and changes the number of loops, n, by one [23], we can write a conservation law

$$\frac{3}{2}\left(\sum_i^n \mathrm{Sl}(A_i) + 2\sum_{i>j}^n \mathrm{Lk}(A_i, A_j)\right) + n = q \bmod 2. \tag{4}$$

Linking numbers are integers with ambiguously defined sign and the number of loops may either increase or decrease by one, hence the modulo 2. This relation is a generalized conservation of topological charge q [12] and reflects the fact that, due to the presence of line defects, only the even or odd parity of q is conserved [12,24]. The interpretation of q as the topological charge can be justified with an example. Consider q homeotropic spherical particles in a planar nematic cell, each with its own Saturn ring loop [2]. Such a system satisfies the above equation as it contains $n = q$ unlinked loops with $\mathrm{Sl} = 0$. Entangled structures can be reached by applying successive tetrahedral rotations, which preserve both the left side of Eq. (4) and the topological charge.

The derived formalism can be demonstrated using our dimer structures. There are two rewiring sites situated symmetrically between the colloidal particles.

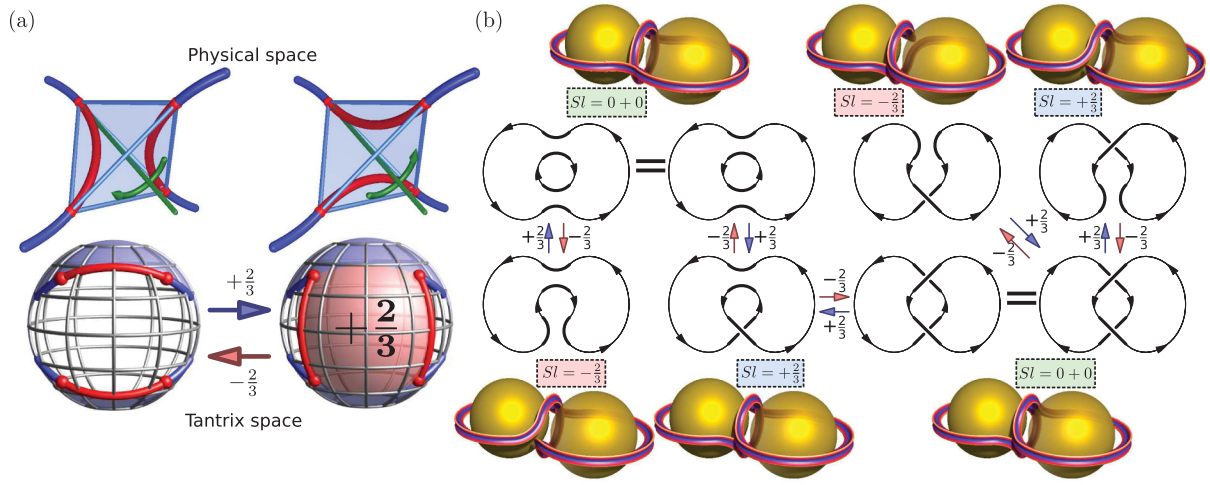

FIG. 3 (color). (a) Tetrahedral rotation changes the positions of two disclination line segments, which also changes the curve, traced by the tangent on the unit sphere. The spherical area traced by this curve changes by $\pm 4\pi/6$ (shown in red), which is directly related to the $\pm 2/3$ change in writhe and consequently, the self-linking number. (b) Schematic depiction of dimer structures and transformations between them. A tetrahedral rotation changes the writhe by $\pm 2/3$ if parametrizations of initial and final structure are the same. By varying the parametrization, we can calculate writhes of all different dimer structures. Depicted here are the theta, chiral omega, and figure-eight structures and the pair of Saturn rings, with their respective self-linking numbers. Structures that consist of two loops are shown with both possible choices of parametrization. Orientations of loop parametrizations are indicated by arrows.

The $3 \times 3 = 9$ possible structures consist of one theta structure, two equivalent structures with disjoint Saturn rings, two equivalent pairs of chiral omega structures, and a pair of chiral figure-eight structures. The theta structure has zero self-linking number and the others are reached by successive tetrahedral rotations. The structures with one loop have self-linking number $\pm 2/3$, while the structures with two loops have both self-linking numbers equal to zero, which agrees with the conservation law (4). The results are shown in Fig. 3(b).

The derived conservation law (4) holds for a set of multiple linked loops as a whole. Individual constituent loops have a self-linking number of the form $p/3$, where p is even if an even number of disclinations pass through the loop and odd in the converse case. This can be shown by choosing an idealized model of a director field representing such loop and determining mathematically which element of the fundamental group the given director field represents [12,24]. The calculation is carried out in [22].

We have shown that any rewiring of two orthogonally crossing $-1/2$ disclinations is possible, as the topological requirements are satisfied entirely by the changes in the self-linking and linking numbers caused by the application of the tetrahedral rotations. In contrast, $+1/2$ disclinations cannot form rich entangled structures, as they only allow integer self-linking numbers. Under the restriction that only $-1/2$ disclinations are present, the self-linking numbers of the loops are topological invariants, coupled with surrounding topological charges by a conservation law. In confined, chiral, and field-affected environments, however, the type of the disclination profile may vary between $\pm 1/2$ and twist disclinations [25]. Our findings do not apply directly to such cases, as the self-linking number is ill-defined if the disclination cross-section does not have constant symmetry.

Our work introduces two important advances in the theoretical understanding of nematic braids. By combining the formalism of differential geometry with the characteristics of nematic defects, we are able to show that the self-linking number is a topological invariant of $-1/2$ disclination loops that successfully differentiates between the loops and ensures the conservation of topological charge. On the other hand, our explanation of local rewiring by tetrahedral rotations gives a qualitative three-dimensional image of disclinations and resolves the behavior of director in complex disclination loop networks seen in experiments and simulations [8,10,13]. The richness of entangled structures increases with the number of available rewiring sites, which are more abundant in chiral systems [4,13]. The rewiring rules classify the set of possible braids and allow a transparent design of new structures and guidance of their experimental realization. Provided symmetry-driven rewiring rules similar to our tetrahedral rotations exist, our formalism can be extended to systems with different line defects, crossing geometries [26], or any system with a well-defined self-linking number (e.g., loop DNA [17,27]).

We thank T. Lubensky and R. Kamien for helpful discussions regarding the topological interpretation of the results. We acknowledge support from the Slovenian Research Agency (research program P1-0099 and project J1-2335) and the NAMASTE Centre of Excellence.

[1] P. Poulin, H. Stark, T. C. Lubensky, and D. A. Weitz, Science **275**, 1770 (1997).
[2] I. Muševič, M. Škarabot, U. Tkalec, M. Ravnik, and S. Žumer, Science **313**, 954 (2006).
[3] C. P. Lapointe, T. G. Mason, and I. I. Smalyukh, Science **326**, 1083 (2009).
[4] N. Hijnen, T. A. Wood, D. Wilson, and P. Clegg, Langmuir **26**, 13 502 (2010).
[5] T. Araki, M. Buscaglia, T. Bellini, and H. Tanaka, Nature Mater. **10**, 303 (2011).
[6] J. D. Joannopoulos, S. G. Johnson, J. N. Winn, and R. D. Meade, *Photonic Crystals: Molding the Flow of Light* (Princeton University Press, Princeton, NJ, 2008), 2nd ed.
[7] M. Ravnik *et al.*, Phys. Rev. Lett. **99**, 247801 (2007).
[8] M. Ravnik and S. Žumer, Soft Matter **5**, 4520 (2009).
[9] S. Žumer, in Book of Abstracts of the 21st International Liquid Crystal Conference, Keystone, Colorado, 2006, Abstract PLEN4-22, p. 16.
[10] T. Araki and H. Tanaka, Phys. Rev. Lett. **97**, 127801 (2006).
[11] M. Ravnik and S. Žumer, Soft Matter **5**, 269 (2009).
[12] N. D. Mermin, Rev. Mod. Phys. **51**, 591 (1979).
[13] U. Tkalec, M. Ravnik, S. Čopar, S. Žumer, and I. Muševič (to be published).
[14] S. Kutter, Ph.D. thesis, University of Cambridge, 2002.
[15] R. D. Kamien, Eur. Phys. J. B **1**, 1 (1998).
[16] F. B. Fuller, Proc. Natl. Acad. Sci. U.S.A. **75**, 3557 (1978).
[17] D. Han, S. Pal, Y. Liu, and H. Yan, Nature Nanotech. **5**, 712 (2010).
[18] W. T. M. Irvine and D. Bouwmeester, Nature Phys. **4**, 716 (2008).
[19] J. E. Avron, D. Osadchy, and R. Seiler, Phys. Today **56**, 38 (2003).
[20] R. D. Kamien, Rev. Mod. Phys. **74**, 953 (2002).
[21] M. A. Berger and C. Prior, J. Phys. A **39**, 8321 (2006).
[22] See supplemental material at http://link.aps.org/supplemental/10.1103/PhysRevLett.106.177801 for background on differential geometry of ribbons and detailed derivation of expressions used in this article.
[23] V. V. Prasolov and A. B. Sossinsky, *Knots, Links, Braids and 3-Manifolds* (American Mathematical Society, Providence, Rhode Island, 1997) p. 32.
[24] K. Jänich, Acta Appl. Math. **8**, 65 (1987).
[25] J. I. Fukuda, Phys. Rev. E **81**, 040701 (2010).
[26] D. Kang, J. E. Maclennan, N. A. Clark, A. A. Zakhidov, and R. H. Baughman, Phys. Rev. Lett. **86**, 4052 (2001).
[27] M. Otto and T. A. Vilgis, Phys. Rev. Lett. **80**, 881 (1998).